Bridging atomistic spin dynamics methods and phenomenological models of single-pulse ultrafast switching in ferrimagnets

Florian Jakobs and Unai Atxitia◉

Dahlem Center for Complex Quantum Systems and Fachbereich Physik, Freie Universität Berlin, 14195 Berlin, Germany

We bridge an essential knowledge gap on the understanding of all-optical ultrafast switching in ferrimagnets, namely, the connection between atomistic spin dynamics methods and macroscopic phenomenological models. All-optical switching of the magnetization occurs after the application of a single femtosecond laser pulse to specific ferrimagnetic compounds. This strong excitation puts the involved degrees of freedom, electrons, lattice, and spins out-of-equilibrium between each other. Atomistic spin models have quantitatively described all-optical switching in a wide range of experimental conditions, while having failed to provide a simple picture of the switching process. Phenomenological models are able to qualitatively describe the dynamics of the switching process. However, a unified theoretical framework is missing that describes the element-specific spin dynamics as atomistic spin models with the simplicity of phenomenology. Here, we bridge this gap and present an element-specific macrospin dynamical model which fully agrees with atomistic spin dynamics simulations and symmetry considerations of the phenomenological models.

I. INTRODUCTION

Since its experimental discovery [1], the theoretical description of laser-induced all-optical switching (AOS) of the magnetization in GdFeCo ferrimagnetic alloys has remained a challenge. Despite intense experimental and theoretical research in the field [1–12], an established and unified picture of the process is still missing. Experimental findings are mostly compared or interpreted in terms of atomistic spin dynamics simulations [13–17], multisublattice spin dynamics based on symmetry arguments [5,18,19], and based on the Landau-Lifshitz-Bloch equation [20–22]. The main goal of the present work is the revision, extension, and merging of these approaches into a unified model.

Atomistic spin dynamics (ASD) models have been used before to quantitatively describe ultrafast dynamics in $3d$ transition metals [23,24] and $4f$ rare-earth ferromagnets [25,26]. They have also been used in GdFeCo to describe the equilibrium thermal properties [13], the thermal character of AOS [4], the so-called transient ferromagneticlike state [3], the demonstration of spin-current-mediated rapid magnon localization and coalescence [27], and the possibility of AOS using picosecond-long laser pulses [16]. Results from atomistic spin models also compare qualitatively well to an analytical theory based on the excitation of spin-wave exchange modes [8], provide insights for optimal electron, phonon, and magnetic characteristics for low-energy switching [28], and predict a maximum repetition rate using two consecutive laser pulses [29]. More sophisticated, orbital-resolved atomistic models provide insights into the role of the intraexchange coupling between $4f$ and $5d$ electrons in the dynamics of GdFeCo alloys [14]. Atomistic models can naturally describe switching in Gd/Fe multilayers composed of very thin layers [30,31].

Recent observations [32,33] of single pulse switching in Mn_2Ru_xGa alloys are also well described by ASD methods [34]. Despite the demonstrated success in modeling AOS, ASD simulation results are cumbersome to interpret without an analytical model that unveils the role of the different processes and interactions during the switching process. This potential semianalytical model has to capture most of the features of the ASD simulations.

Semiphenomenological models describing switching already exist. A macroscopic theory for the description of the dynamics and relaxation of the macroscopic (sublattice) magnetization of ferromagnets and antiferromagnets was developed originally by Baryakhtar [9,35]. An extension of such phenomenology to ferrimagnets in the context of ultrafast spin dynamics was introduced in Ref. [5]. At the ultrafast scale, magnetization dynamics are dominated by atomic scale spin excitations; these spin dynamics are driven by dissipative processes which in ferrimagnets are twofold, relativistic and exchange driven. Relativistic processes allow for the exchange of angular momentum between the spins and lattice degree of freedom due to the presence of spin-orbit interaction connecting them. Exchange processes can arise due to the transport of spin angular momentum—spin and magnon transport—which is the only means to exchange angular momentum in ferromagnets. In multisublattice magnets, another, different pathway opens, namely, the local exchange of angular momentum. To account for such local exchange processes in ferrimagnets, the equation of motion for the magnetization dynamics proposed by Landau and Lifshitz [36] is enhanced by an exchange-relaxation term [5,9,19,37]. Within this macroscopic model, the exchange relaxation dominates the dynamics when the magnetic sublattices are driven into mutual nonequilibrium. Qualitative agreement to

experiments in two-sublattice magnets has been demonstrated [19], such as AOS in ferrimagnetic GdFeCo using fs laser pulses [5] and ps laser pulses [38], AOS in Heusler semimetals Mn_2Ru_xGa [39], or element-specific demagnetization of ferromagnetic NiFe alloys [18]. Quantitative comparison of this model to neither experiments nor ASD simulations have been conducted so far. While the arguments behind such phenomenology are robust, the range of applicability and the validity of the model parameters could be questioned. For instance, the parameters defining the relativistic and exchange relaxation are assumed to be constant and of the same order. The magnetic free-energy functional is calculated for near-thermal equilibrium states. This implies a relatively strong coupling to the heat bath, while switching conditions are supposedly fulfilled when the exchange relaxation between sublattices dominates over the relaxation to the heat bath.

An alternative macroscopic model directly derived from an atomistic spin model has also been proposed. This model is based in the Landau-Lifshitz-Bloch (LLB) equation of motion [20,40–43]. The LLB model for two-sublattice magnets [20,42] has been used in the context of AOS in GdFeCo, e.g., the element-specific demagnetization rates compare well to experiment, and it predicts that near the magnetic phase transition, the otherwise slower Gd sublattice becomes faster than Fe [22], as recently observed [44]. The LLB model has been demonstrated to provide accurate analytical expressions for the temperature dependence of the relativistic relaxation parameter as well as for the nonequilibrium effective fields below and above the critical temperature [42]. Moreover, the LLB model also describes the transverse motion of the magnetization. This makes it the preferred model for computer simulations of heat-assisted magnetic recording [45] and realistic description of all-optical switching [46], and ultrafast spintronics, such as domain-wall motion [47,48] or skyrmion creation by ultrafast laser pulses [49]. So far, the LLB model and Baryakhtar-like models have been considered as complementary approaches. Here, we merge them into one unified approach.

In this work, we address the issues discussed above by directly comparing both phenomenological models to ASD simulations. We do so since ASD simulations have already been quantitatively compared to experiments in the literature. We find that quantitative comparison between ASD and both phenomenological models is partially possible for laser excitation producing small deviation from equilibrium. However, those models hardly reproduce magnetic switching using the same parameter values describing the relaxation of small perturbations. Here, based upon those phenomenological models, we propose a macroscopic model that compares precisely to the magnetization dynamics calculated using ASD simulations, including element-specific magnetization relaxation and switching. This model bridges atomistic spin dynamics based models and previously proposed phenomenological models. Notably, it provides a deeper understanding to the parameters entering the phenomenological models and sheds some light into the process of ultrafast switching in ferrimagnets.

The work is broken down in the following way: In Sec. II, we present the atomistic spin model for the calculation of the

magnetic equilibrium properties and nonequilibrium dynamics. The equilibrium properties are compared to a mean-field model. We then provide atomistic calculations of the ultrafast magnetization dynamics with input from the two-temperature model. These results are the basis for the comparison to the phenomenological models presented in Sec. III. First, we present the Baryakhtar model and the Landau-Lifshitz-Bloch model. Second, we compare the ultrafast magnetization dynamics calculated with those models to the atomistic spin dynamics results. Finally, in Sec. III C, we present the unified phenomenological model, a hybrid model combining Baryakhtar and LLB models, and its comparison to atomistic spin dynamics.

II. ATOMISTIC SPIN MODEL

Ferrimagnetic materials are characterized by spontaneous magnetization as a result of two or more components of nonparallel magnetic moments [50]. Atomistic spin models based on the Heisenberg Hamiltonian can be considered one of the simplest microscopic models able to reproduce the equilibrium properties of ferrimagnets. The spin system energy due to only the exchange interactions can be described by an effective Heisenberg model,

$$\mathcal{H} = -\sum_{i \neq j} J_a \mathbf{S}_{a,i} \cdot \mathbf{S}_{a,j} - \sum_{i \neq j} J_b \mathbf{S}_{b,i} \cdot \mathbf{S}_{b,j} - \sum_{i \neq j} J_{ab} \mathbf{S}_{a,i} \cdot \mathbf{S}_{b,j},$$

(1)

where $J_{a(b)(ab)}$ is the exchange constant between neighboring sites represented by two classical spin vectors $\mathbf{S}_i$ and $\mathbf{S}_j$ ($|\mathbf{S}| = 1$). Further, we include magnetic anisotropy terms in Eq. (1) to set a preferential axis for the magnetization to switch about. However, since the anisotropy energy is relatively low in comparison to the exchange energy, at the picosecond timescale it plays a marginal role in the switching process. This makes for a simpler Hamiltonian and a more direct comparison to the phenomenological models. To model a ferrimagnet, one needs to consider two alternating sublattices of unequal and antiparallel moments, with three exchange coupling constants: ferromagnetic for each sublattice (J_a and J_b) and a third for the antiferromagnetic interaction between them, J_{ab}. For instance, GdFeCo alloys are composed of a transition-metal FeCo and Gd rare-earth sublattices. We model the Fe and Co spins as only one magnetic sublattice, and we assume a common atomic magnetic moment of $\mu_{FeCo} = 1.94\mu_B$. In these alloys, the rare-earth impurities add localized $4f$ spins to the system assumed to be $\mu_{Gd} = 7.6\mu_B$. The amorphous nature of GdFeCo is modeled by using a simple cubic lattice model, but with random placements of Gd moments within the lattice to the desired concentration. The applicability of the Heisenberg approximation relies on the stability of local moments under rotation and at high temperature where Stoner excitations are generally weak [51]. It is assumed that the electronic properties are temperature independent in the range where the system is magnetically ordered.

A. Atomistic spin dynamics

Equilibrium and nonequilibrium element-specific magnetic properties of a ferrimagnet are calculated using atomistic

spin dynamics simulations which are based in the stochastic-Landau-Lifshitz-Gilbert equation (s-LLG) [52],

$$\left(1 + \lambda_i^2\right)\mu_{s,i}\dot{\mathbf{S}}_i = -\gamma\mathbf{S}_i \times [\mathbf{H}_i - \lambda_i\left(\mathbf{S}_i \times \mathbf{H}_i\right)], \qquad (2)$$

where γ is the gyromagnetic ratio and λ_i is the so-called phenomenological sublattice-specific damping parameter. By including a Langevin thermostat, the spin dynamics including statistical—equilibrium and nonequilibrium thermodynamic—properties can be obtained. An effective fieldlike stochastic term $\boldsymbol{\zeta}_i$ is added to the effective field $\mathbf{H}_i = \boldsymbol{\zeta}_i(t) - \frac{\partial\mathscr{H}}{\partial\mathbf{S}_i}$, with white-noise properties [53]: $\langle\boldsymbol{\zeta}_i(t)\rangle = 0$ and $\langle\boldsymbol{\zeta}_i(0)\boldsymbol{\zeta}_j(t)\rangle = 2\lambda_i k_\mathrm{B}T\mu_{s,i}\delta_{ij}\delta(t)/\gamma$. The variance of the Langevin noise is chosen such that the fluctuation-dissipation theorem is fulfilled.

B. Mean-field approximation

Exact analytical expressions for the $M(T)$ curve are cumbersome to derive due to the many-body character of the problem. Here we resort to the mean-field approximation (MFA), already used in previous works [8,13,54]. We note that to be able to apply the MFA for the GdFeCo impurity model, and thus translation nonsymmetric with respect to spin variables $\mathbf{S}_i$, we need to transform the Heisenberg Hamiltonian to a symmetric one. We use the spin analogy of the virtual crystal approximation (VCA) to transform the disordered lattice Hamiltonian $\mathscr{H}$ to a symmetric VCA Hamiltonian $\mathscr{H}_\mathrm{VCA}$. Within the VCA, we evaluate the effective sublattice exchange parameters, given by the sum of the exchange interactions of a given spin at a site $\mathbf{r}_i$ of sublattice i with all other atoms of this sublattice. This involves weighting the exchange parameters by the relative composition, $x_i \equiv$ concentration species i [8],

$$J_i = \sum_{\mathbf{r}_i,\mathbf{r}_i'}J(\mathbf{r}_i,\mathbf{r}_i')\underbrace{\equiv}_{\mathrm{VCA}}x_iJ(\mathbf{r}_i,\mathbf{r}_i') \quad \text{intrasublattice}, \qquad (3)$$

whereas the intersublattice effective exchange reads

$$J_{ij} = \sum_{\mathbf{r}_i,\mathbf{r}_j'\notin A_i}J(\mathbf{r}_i,\mathbf{r}_j')\underbrace{\equiv}_{\mathrm{VCA}}x_iJ(\mathbf{r}_i,\mathbf{r}_j') \quad \text{intersublattice}. \qquad (4)$$

Thus the VCA Hamiltonian reads

$$\mathscr{H}_\mathrm{VCA} = \sum_{j\in A_i}J_i\mathbf{S}_i\cdot\mathbf{S}_j + \sum_{j\notin A_i}J_{ij}\mathbf{S}_i\cdot\mathbf{S}_j, \qquad (5)$$

where A_i represent the magnetic sublattice of the spin $\mathbf{S}_i$. In the exchange approximation, we define the MFA field as

$$\mu_a H_a^\mathrm{MFA} = z_aJ_{aa}m_a + z_{ab}J_{ab}m_b. \qquad (6)$$

The element-specific equilibrium magnetization is calculated via the self-consistent solution of $m_a = L(\beta\mu_aH_a^\mathrm{MFA})$ and $m_b = L(\beta\mu_bH_b^\mathrm{MFA})$. z_a and z_{ab} correspond to the number of first-nearest neighbors of type a and b, respectively. It is well known that the MFA overestimates the value of the critical temperature T_C. However, a very good agreement between ASD and MFA can be obtained by using a reduced value for the exchange parameters, even for multilattice magnets [54]. Figure 1 shows element-specific $M_a = x_a\mu_am_a(T)$ using ASD simulations and renormalized MFA for $x_\mathrm{Gd} = 25\%$.
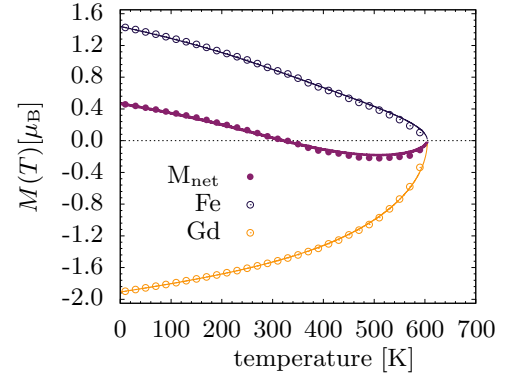

FIG. 1. Equilibrium magnetization of a GdFeCo alloy for Gd concentration, $x_\mathrm{Gd} = 25\%$. Element-specific normalized equilibrium magnetization and net equilibrium magnetization, $M(T) = x_\mathrm{Gd}\mu_\mathrm{Gd}m_\mathrm{Gd} - x_\mathrm{Fe}\mu_\mathrm{Fe}m_\mathrm{Fe}$, where $\mu_\mathrm{Gd(Fe)}$ is the atomic magnetic moment of Gd(Fe). Lines correspond to the mean-field approximation with renormalized exchange parameters. Symbols correspond to atomistic spin dynamics simulations.

Net magnetization is also shown in Fig. 1, which is defined as $M(T) = x_\mathrm{Gd}\mu_\mathrm{Gd}m_\mathrm{Gd} - x_\mathrm{Fe}\mu_\mathrm{Fe}m_\mathrm{Fe}$. The agreement between ASD and MFA is good enough for all the temperature regions. We observe the presence of compensation temperature T_M at room temperature for $x_\mathrm{Gd} = 25\%$ at which the thermally averaged magnetization of both sublattices is equal but opposite, so that the magnetization of the system is equal to zero, $M(T_\mathrm{M}) = 0$. The mapping of the atomistic spin model and the corresponding mean-field approximation turns out to be necessary for a quantitative comparison to the phenomenological models, and thereby paramount for the unification of both pictures.

C. Two-temperature model

Single-pulse all-optical switching has been demonstrated to be a thermal process in ferrimagnetic GdFeCo alloys [4] and in Mn_2Ru_xGa Heusler semimetals [32]. Ultrafast heating by optical or electric means is sufficient to achieve switching in specific GdFeCo alloys [55]. Although the minimum achievable duration of the electric pulses is limited to picoseconds, those are better suited for potential integration into applications. Laser pulses can be as short as only a few femtoseconds, which permits it to excite the electron system in timescales of the order of the exchange interaction, allowing for the investigation of fundamental physics governing switching. In this work, we center on excitation of the ferrimagnetic GdFeCo using femtosecond laser pulses. When a metallic ferrimagnetic thin film is subjected to a near-infrared laser pulse, only the electrons are accessible by the photon electric field. Initially, the absorbed energy is barely transferred to the lattice and, consequently, the electron system heats up. The electron and phonon temperatures are decoupled for up to several picoseconds until the electron-phonon interaction equilibrates the two heat baths. This phenomenology is well captured by the so-called two-temperature model (2TM) [56,57], which can be written as two coupled differential
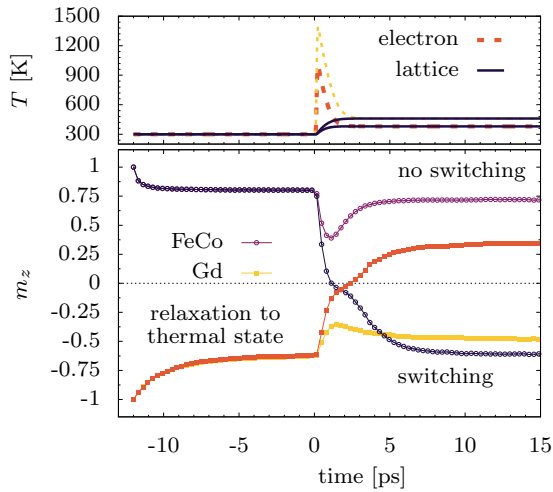
FIG. 2. (a) Electron and lattice temperature dynamics for two laser pulse power values, P_0 and $2P_0$. Both electron and lattice temperature are kept constant, $T = 300$ K, for $t < 0$. At $t = 0$, a laser pulse is applied and the dynamics of the electron and lattice temperature heat up. The dynamics of those temperatures are theoretically described by the two-temperature model. (b) Element-specific magnetization dynamics induced by the heat profile at (a). The dynamics are calculated using atomistic spin dynamics methods. For lower laser powers P_0, the magnetization of both sublattices demagnetizes rapidly and remagnetizes towards the new equilibrium. For laser power $2P_0$, the magnetization of both sublattices demagnetizes and switches. After switching, they relax towards the thermal equilibrium state. GdFeCo alloys with $x_{Gd} = 25\%$ are calculated.

equations,

$$C_{el} \frac{\partial T_{el}}{\partial t} = -g_{ep}(T_{el} - T_{ph}) + P_l(t), \quad (7)$$

$$C_{ph} \frac{\partial T_{ph}}{\partial t} = +g_{ep}(T_{el} - T_{ph}). \quad (8)$$

Here, $C_{el} = \gamma_{el} T_{el}$, where $\gamma_{el} = 6 \times 10^2$ J/m^3 K^2, and $C_{ph} = 3.8 \times 10^6$ J/m^3 K represent the specific heat of the electron and phonon system. The electron-phonon coupling is taken to be temperature independent, $G_{ep} = 7 \times 10^{17}$ J/m^3 K. Here, $P(t)$ is a Gaussian-shaped pulse with a duration of 55 fs. The exact values of the parameters entering the 2TM in GdFeCo are still unknown. The values we use here are close to those commonly used, e.g., in Refs. [4,8,34].

D. Ultrafast magnetization dynamics using ASD

Element-specific magnetization dynamics induced by a femtosecond laser pulse are calculated by combining the atomistic s-LLG equation for the spin dynamics [Eq. (2)] and the 2TM for the electron temperature [Eq. (7)]. The electron system acts as a heat bath for the atomic spins. We consider a lattice with $N = 50 \times 50 \times 50$ spins, and damping parameters $\lambda_{Gd} = 0.01 = \lambda_{Fe}$. Figure 2 shows, for $t < 0$, the dynamics of the element-specific magnetization from an initial saturated state ($T = 0$ K), towards thermal equilibrium with the heat bath which is set to $T = 300$ K. The relaxation dynamics of the Fe sublattice is faster than those of the Gd sublattice. This comes out naturally as the element-specific

dissipation of angular momentum scales as $\dot{m}_z \sim \gamma \lambda / \mu_s$ in the Gd sublattice ($\mu_{Gd} = 7.6 \mu_B$) is slower than in the Fe sublattice ($\mu_{Fe} = 1.94 \mu_B$). Once the magnetic system is in thermal equilibrium with the heat bath, we apply the laser pulse $t > 0$, which introduces energy into the electron system and induces ultrafast magnetization dynamics. To illustrate the switching and no-switching dynamics, we consider two limiting cases: dynamics induced by low laser power P_0 and large laser power $2P_0$. The electron temperature increases up and above the Curie temperature in timescales of a few hundreds of femtoseconds; see Fig. 2(a). This reflects in the magnetic system as a fast demagnetization of both the Fe and Gd sublattices. For relatively low laser power P_0, the magnetization of both sublattices reduces while the electron temperature remains relatively high. Once the electron temperature reduces and equalizes to the lattice temperature, they can be considered to be in a new, thermal quasiequilibrium. The magnetization recovers to the thermal state given by the heat-bath temperature, which is higher than it initially was ($T = 300$ K). This is why the final magnetization value is smaller than the initial one. For higher laser powers $2P_0$, the magnetization of both sublattices reduces quickly. The Fe sublattice is faster than the Gd one. Once the magnetization of the Fe sublattice hits zero, instead of remaining demagnetized, the magnetization starts to develop toward the opposite direction, while the magnetization of the Gd sublattice is still in the process of demagnetization. During a couple of picoseconds, both sublattice magnetizations are aligned along the same direction, similar to a ferromagnet. Consequently, this nonequilibrium state has been named the transient ferromagneticlike state [3]. One can observe in Fig. 2(b) that the demagnetization rates of both sublattices slow down when the Fe magnetization crosses zero. This change reveals the set in of a process driving the magnetization dynamics different from the one driving the initial demagnetization. It has been argued that at this point, direct exchange of angular momentum between sublattices dominates over processes of relativistic origin, which in turn dissipate angular momentum into the heat bath. Interestingly, soon after switching, both sublattice magnetizations rapidly relax to equilibrium, indicating that relaxation into the heat bath dominates the dynamics.

III. PHENOMENOLOGICAL MODELS

Differently from ASD simulations, phenomenological models describe the element-specific magnetization dynamics by solving two coupled equations of motion, one for each sublattice. In this work, we aim to find a phenomenological model that describes the same element-specific magnetization dynamics as those coming out from the ASD simulations (Fig. 2). The starting point is the comparison of the ASD simulations to well-known phenomenological models. We show that those models are unable to describe in a satisfactory way the different element-specific magnetization dynamics studied in the previous section and summarized in Fig. 2.

A. Baryakhtar model

The simplest model to describe element-specific magnetization dynamics and switching in ferrimagnets was proposed

by Mentink and co-workers [5]. Longitudinal spin dynamics was derived from Onsager's relations,

$$\frac{\mu_a}{\gamma_a}\frac{dm_a}{dt} = \alpha_a^B \mu_a H_a + \alpha_e^B(\mu_a H_a - \mu_b H_b), \qquad (9)$$

$$\frac{\mu_b}{\gamma_b}\frac{dm_b}{dt} = \alpha_b^B \mu_b H_b + \alpha_e^B(\mu_b H_b - \mu_a H_a), \qquad (10)$$

where $\alpha_{a,b}^B$ stands for the relaxation parameter of relativistic origin, which dissipates angular momentum out of the spin system, and α_e^B stands for the exchange-relaxation parameter and describes the rate of dissipation of angular momentum between sublattices. By construction, exchange relaxation conserves the total angular momentum. We emphasize here the difference in the notation between the atomic relaxation parameter λ, describing the dissipation of the atomic spins in ASD simulations, and the macrospin relaxation parameter α, describing the dissipation of the whole magnetic sample. Within this model, the values for $\alpha_{a,b}^B$ and α_e^B are unknown, but used as fitting parameters when compared to experiments. The internal effective field $H_{a(b)}$, acting on sublattice $a(b)$, is derived from a nonequilibrium mean-field approximation,

$$\mu_a H_a = -\beta^{-1} L^{-1}(m_a) + \mu_a H_a^{MFA}, \qquad (11)$$

where $L^{-1}(x)$ is the inverse Langevin function, and $\beta = 1/k_B T$, where T represents the temperature of the heat bath to which the spin system is coupled. At equilibrium, the effective field is $H_a = 0$, as $m_a = L(\beta \mu_a H_a^{MFA})$. The same arguments apply for sublattice b. It turns out that by solving Eqs. (9) and (10) together with the 2TM, described in Eqs. (7) and (8), one obtains similar ultrafast magnetization dynamics as those using ASD simulations (Fig. 2). Element-specific demagnetization [18] and switching dynamics [19] based on this approach have been discussed thoroughly before. In those works, the values for the relaxation parameters, relativistic and exchange, are taken constant and of the same order, $\alpha_{Fe}^B \approx \alpha_{Gd}^B \approx \alpha_e^B$. We note that here α_a^B defines the rate of change of the angular momentum $(m\mu/\gamma)$. It differs from the definition of intrinsic damping parameters in ASD, which are related to the rate of change of the magnetization (m). Similarly to ASD methods though, within the Baryakhtar model, the observed fast dynamics of the Fe sublattice is related to a smaller value of atomic magnetic moment.

The switching process within the Baryakhtar-like model is explained in the following manner. Since the Fe sublattice reacts faster than Gd to heating, it is expected to remain closer to thermal equilibrium with the heat bath. This translates into a smaller nonequilibrium effective field acting on Fe than in Gd, $H_{Fe} \ll H_{Gd}$, during the action of the laser pulse. For strong enough pulses, the Fe magnetization rapidly reduces, $m_{Fe} \approx 0$; still, H_{Fe} is small in comparison to H_{Gd}, in a way that the dynamics of Fe can be fairly approximated by $\dot{m}_{Fe} \approx \alpha_e^B H_{Gd}$. This drives the magnetization of Fe towards the opposite direction. The field H_{Gd} is defined by the energy of the system, H_{Gd}^{MFA} [Eq. (6)] and α_e^B from the coupling between the Gd and the Fe sublattices. After switching, $H_{Fe} \approx H_{Gd}$ and relativistic relaxation processes dominate the dynamics and drive magnetization to complete the switching. The question here is to what extent the nonequilibrium fields, as given by
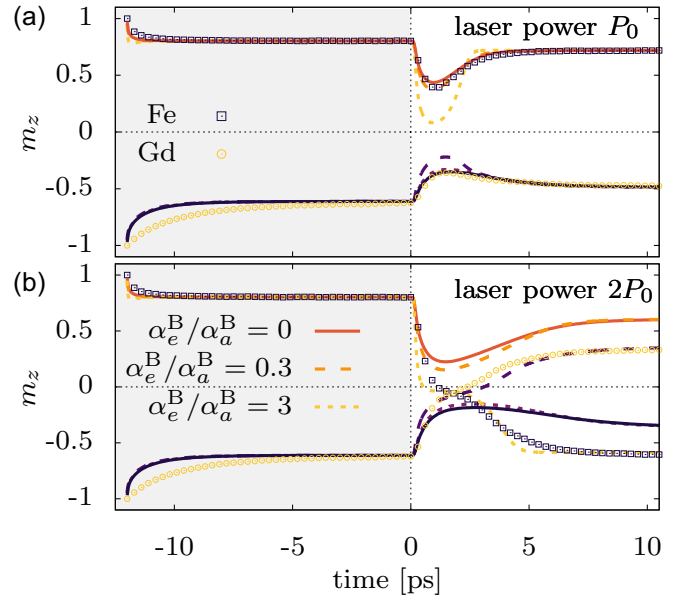

FIG. 3. Element-specific magnetization dynamics of GdFeCo calculated using atomistic spin dynamics (symbols) and macroscopic Baryakhtar-like equation (solid lines) for two laser pulse power values (a) P_0 and (b) $2P_0$. Both electron and lattice temperature are kept constant, $T = 300$ K, for $t < 0$. At $t = 0$, a laser pulse is applied. In the Baryakhtar-like model, the relativistic relaxation parameters α_a^B have a value different from the Gilbert damping in ASD simulations, $(\gamma/\mu_{Fe})\alpha_{Fe}^B = 0.005$ and $(\gamma/\mu_{Gd})\alpha_{Gd}^B = 0.01$. The exchange-relaxation parameter is varied, $\alpha_e^B/\alpha_{Fe}^B = 0, 0.3$, and 3. The relaxation to the thermal state ($t < 0$) is only well described for the Fe sublattice. (a) For P_0, the laser-induced dynamics is well described by $\alpha_e^B/\alpha_{Fe}^B = 0.1$. (b) For $2P_0$, the demagnetization phase of both sublattices is relatively well described in comparison to ASD simulations. Switching is also possible; here, for instance, for a value $\alpha_e^B/\alpha_{Fe}^B = 3$.

Eq. (11), are accurate and how the relaxation parameters are related to the atomic damping parameters in ASD.

So far the connection between the relaxation parameters in the ASD and Baryakhtar-like model is unknown. In ASD simulations, shown in Fig. 2, we have used $\lambda_{Fe} = \lambda_{Gd} = 0.01$ as the atomistic relaxation parameter. One would expect that the relaxation parameters in the atomistic and macroscopic models are related as $\lambda_a \approx \alpha_a^B(\gamma_a/\mu_a)$. In an attempt to find this correspondence, we directly compare results from ASD simulations and Baryakhtar-like models for different values of α_a^B and α_e^B in Eqs. (9) and (10). We numerically solve Eqs. (9)–(11) coupled to the 2TM with exactly the same parameters as for the ASD simulations. After exploring the results of the Baryakhtar model for a range of values for α_a^B and α_e, we find that for some values, the agreement is good, as one observes in Fig. 3; however, it is not possible to find a good match for all scenarios.

In order to illustrate this, we first focus on the dynamics induced by the laser pulse with power P_0 [Fig. 3(a)]. We find a good match for the laser-induced magnetization dynamics [$t > 0$ for $(\gamma/\mu_{Fe})\alpha_{Fe} = 0.005$ and $(\gamma/\mu_{Gd})\alpha_{Gd} = 0.01$] and for values of exchange relaxation of up to $\alpha_e^B/\alpha_{Fe}^B = 0.3$. For values $\alpha_e^B/\alpha_{Fe}^B < 0.3$, thermal relaxation ($t < 0$) of the Fe is

also well described, however, the relaxation of the Gd sublattice is significantly faster. For larger values of the exchange relaxation, $\alpha_e^B/\alpha_{Fe}^B = 3$, the dynamics of both sublattices are substantially sped up and strongly disagree with the ASD simulations.

For larger laser pulse power $2P_0$, the magnetization switches using ASD simulations. We keep the same values for the relaxation parameters in the Baryakhtar-like model as for P_0, and compare to the ASD simulations. For small values of α_e^B [Fig. 3(b)], differently from the P_0 case [Fig. 3(a)], the dynamics described by the Baryakhtar-like model is not only slower than those of ASD simulations, but it hardly reproduces magnetization switching. In order to reproduce switching, we need to use larger values of the exchange-relaxation parameter, $\alpha_e^B/\alpha_{Fe}^B = 3$. These findings are in agreement with previous works using a Baryakhtar-like model where switching was reproduced for comparable values of α_e^B. However, as we have discussed before, for those values of α_e^B, thermal relaxation dynamics ($t < 0$) is much faster than in ASD simulations. This brings us to the following questions: How much understanding about switching can we gain by using this bare Baryakhtar-like model? Are we missing something?

B. The Landau-Lifshitz-Bloch model

Since the Baryakhtar-like model is based on symmetry arguments, the macroscopic magnetization dynamics coming out from the ASD simulations should also be described by that model with adequate expression for the relaxation parameters and nonequilibrium effective fields. The magnetization dynamics coming out from the ASD simulations is well described by the LLB equation of motion,

$$\frac{dm_a}{dt} = \Gamma_{\parallel,a}(m_a - m_{0,a}), \qquad (12)$$

where

$$\Gamma_{\parallel,a} = 2\lambda_a \frac{\gamma}{\mu_a} k_B T \frac{1}{\xi_a} \frac{L(\xi_a)}{L'(\xi_a)}, \qquad (13)$$

with $\xi_a = \beta \mu_a H_a^{MFA}$, where H_a^{MFA} is given in Eq. (6), and $m_{0,a} = L(\xi_a)$. The same equation applies to the second sublattice b. Here, the relaxation rate $\Gamma_{\parallel,a}$ depends nonlinearly on the nonequilibrium sublattice magnetization $m_{a(b)}$ through the parameter ξ_a. We note that Eq. (12) can be expanded around equilibrium for small perturbations of the magnetization. By doing so, the relaxation rates and effective fields are expressed in terms of equilibrium properties such as equilibrium magnetization and zero-field susceptibilities [20]. In the present work, however, we use the version in Eq. (12). Direct comparison between ASD simulations and the LLB model of element-specific magnetization dynamics is possible and with relatively good agreement. Importantly, since the LLB model is derived directly from the ASD microscopic model, the damping parameters $\lambda_{a(b)}$ in Eqs. (13) and (2) stand for the same physics, i.e., the rate of angular momentum dissipation of the atomic spins. Differently from the Baryakhtar model where $\alpha_{a(b)}^B$ is taken as a fitting parameter, within the LLB model, the value of $\lambda_{a(b)}$ in Eq. (13) is the same as in the ASD simulations. A key difference between the Baryakhtar-like model and the LLB model is that in the latter, an exchange-relaxation term is missing. In order to find a meeting point between these phenomenological models, we rewrite Eq. (12) in terms of a damping term multiplied by an effective field,

$$\frac{dm_a}{dt} = \frac{2\lambda_a L(\xi_a)}{\xi_a} \frac{\gamma}{\mu_a} \frac{m_a - m_{0,a}}{\beta L'(\xi_a)} = \gamma \alpha_a H_a, \qquad (14)$$

where

$$\alpha_a = 2\lambda_a \frac{L(\xi_a)}{\xi_a}. \qquad (15)$$

Differently from the Baryakhtar-like model, in the LLB model, the relaxation parameter strongly depends on temperature and nonequilibrium sublattice magnetization through the thermal field, $\xi_a = \beta \mu_a H_a^{MFA}$. At the same time, the nonequilibrium fields $\mu_a H_a$ within the LLB and Baryakhtar-like models differ. The effective field in the LLB model is defined as

$$\mu_a H_a = \frac{(m_a - m_{0,a})}{\beta L'(\xi_a)}. \qquad (16)$$

Equation (16) provides a microscopic description of the effective field driving the magnetization dynamics in ferrimagnets, based on the Heisenberg spin model [Eq. (1)]. Under the assumption of small perturbations around the equilibrium, both the LLB and Baryakhtar-like effective fields simplify to Landau-like expressions [19]. Equation (14) describes, with a very good degree of accuracy, the relaxation of the angular momentum via dissipation to the heat bath, which corresponds to the relativistic term in Eqs. (9) and (10). Previously, it has been found that ASD simulations compare well to Eq. (14) for coupling parameters of $\lambda_a \approx 0.1$–1 [20,42]. These values can be considered to correspond to the intermediate-to-high coupling regime. Direct comparison between ASD simulations and experiments of single-pulse switching in GdFeCo has suggested values of $\lambda_{Fe} \approx 0.06$ and $\lambda_{Gd} \approx 0.01$ [16]. In the context of the present work, we find that Eq. (14) relatively well describes the thermal relaxation dynamics in direct comparison to ASD simulations (Fig. 4).

In order to account for the exchange relaxation in the LLB model, we follow the Baryakhtar-like model [(9) and (10)] and add an exchange-relaxation term to Eq. (14),

$$\frac{dm_a}{dt} = \gamma \alpha_a H_a + \gamma \frac{\alpha_e}{\mu_a}(\mu_a H_a - \mu_b H_b), \qquad (17)$$

where α_e is a phenomenological exchange-relaxation parameter to be determined by comparison to ASD dynamics. The inclusion of the exchange relaxation (second term on right-hand side) in the LLB improves the agreement with the ASD simulations. With this addition, the LLB model describes well the thermal relaxation for small values of the ratio α_e/α_a, as demonstrated in Fig. 4. For large values of α_e, the LLB model is unable to describe the thermal relaxation dynamics [$t < 0$ in Figs. 4(a) and 4(b)]. For laser power P_0 [Fig. 4(a) ($t > 0$)], the magnetization dynamics is slightly slower using the LLB model than those gained by ASD simulations for $\alpha_e/\alpha_a = 0$. For $\alpha_e/\alpha_a = 0.1$, the agreement is even better than without exchange relaxation. The agreement vanishes when the exchange relaxation is increased to $\alpha_e/\alpha_a = 1$. Critically, when the laser power is increased from P_0 to $2P_0$, for
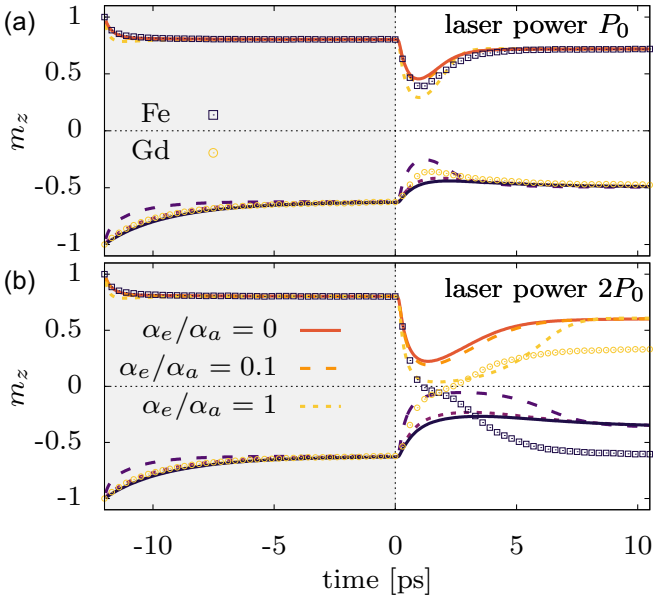
FIG. 4. Element-specific magnetization dynamics of GdFeCo calculated using atomistic spin dynamics (symbols) and macroscopic LLB equation (solid lines) for two laser pulse power values (a) P_0 and (b) $2P_0$. For $t < 0$, the electron and lattice temperatures are $T = 300$ K, and at $t = 0$, a laser pulse is applied. The exchange-relaxation parameter is varied, $\alpha_e/\alpha_a = 0, 0.1$, and 1, where $\alpha_a = 0.01$ and $a =$ FeCo or Gd. The initial relaxation dynamics is well described by $\alpha_e/\alpha_a = 0$. (a) For laser power P_0, the element-specific dynamics is well described for $\alpha_e/\alpha_a = 0.1$. (a) For $\alpha_e/\alpha_a = 1$, exchange relaxation dominates and the element-specific dynamics are similar. (b) For laser power $2P_0$, the switching dynamics is not described by the LLB model.

which ASD simulations show ultrafast switching, the LLB model only shows demagnetization-remagnetization of both sublattices. We find some agreement on the demagnetization timescales when a quite large exchange relaxation is used, $\alpha_e/\alpha_a = 1$. These dynamics are similar to those observed using the Baryakhtar-like model for intermediate values of the exchange-relaxation parameter (Fig. 3). It has been previously demonstrated that by including the transverse components of the equation of motion, switching is possible via a precessional path when a canting between the magnetization of each sublattice exists [21]. Here, we restrict to purely longitudinal switching within the LLB model.

C. Unified phenomenological model

So far, we have constructed a phenomenological model based on the LLB and Baryakhtar-like models, where the dynamics is given by Eq. (17), the effective field by Eq. (16), and the relativistic relaxation parameter by Eq. (15). We still need an expression for the exchange-relaxation parameter. We construct this expression starting with single-species ferromagnets, where sublattices a and b represent the same spin lattice, and hence the exchange of angular momentum is nonlocal. Therefore, $\mu_a H_a - \mu_b H_b = \mu_a H_{ex} a_0^2 \Delta m_a$, with a_0 representing the lattice constant. Hence, the rate of nonlocal angular momentum transfer reads $\Gamma_{ex}^{nonloc.} = \alpha_{ex}(\mu_a H_a - \mu_b H_b) = \alpha_a(A/M_a(T))\Delta m_a$, where A is the so-called micro-
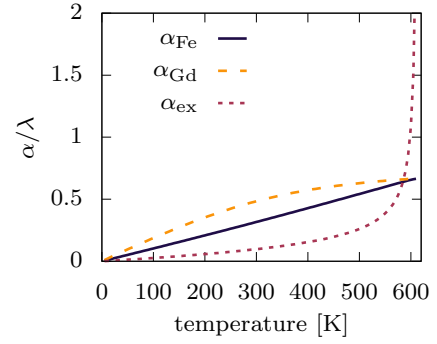

FIG. 5. Thermal equilibrium value of the relativistic exchange parameters α_{Fe} and α_{Gd} and the exchange-relaxation parameter α_{ex} as a function of temperature.

magnetic exchange stiffness [58]. $M_a(T) = (\mu_a/\upsilon_a)m_a$ is the magnetization density at temperature T, where υ_a is the unit-cell volume. Therefore, we find that $\alpha_{ex} = \alpha_a/(zm_a)$, where z is the number of nearest neighbors. By considering that the exchange-relaxation rate should conserve the symmetry under the exchange of the lattice index, $\alpha_{ex}(M_1, M_2) = \alpha_{ex}(M_2, M_1)$, we find that

$$\alpha_{ex} = \frac{1}{2}\left(\frac{\alpha_a}{z_{ab}m_a} + \frac{\alpha_b}{z_{ba}m_b}\right). \tag{18}$$

This expression is the extension of the nonlocal exchange relaxation in ferromagnets to local exchange relaxation in ferrimagnets. This explicit expression for the exchange-relaxation parameter in Eq. (18) completes our unified model, which bridges the atomistic spin dynamics model and the Baryakhtar and LLB macroscopic models.

The previously discussed phenomenological models have introduced the relaxation parameters at a purely phenomenological level (Baryakhtar) or missed to include the exchange relaxation (LLB). Contrary to this, our unified model overcomes this shortcoming, by providing expressions for the relativistic and exchange-relaxation parameters as a function of the sublattice specific atomic relaxation parameter $\lambda_{a(b)}$, through Eqs. (15) and (18), and normalized magnetization $m_{a(b)}$. We note that in our unified model, the values of the relaxation parameters are given by the system parameters and do not depend on the power of the laser fluence. For all laser fluences, the expressions and values are exactly the same; however, due to their dependence on the system temperature and element-specific magnetization, upon photoexcitation with the laser pulse, the values of the relaxation parameters will change dynamically. For large laser powers, the exchange-relaxation parameter becomes of the same order or even larger than the relativistic relaxation parameter. In the previous phenomenological models, the exchange-relaxation constant needed to have a large value in order to describe switching. By contrast, in order to describe low laser power dynamics, the exchange-relaxation constant needed to have a relatively small value ($\alpha_{ex}/\alpha_{a(b)} \ll 1$) (Fig. 3). The expression for the exchange-relaxation parameter that we propose in Eq. (18) captures this behavior naturally.

Figure 5 shows the equilibrium value of the relativistic exchange parameters (α_{Fe} and α_{Gd}) and the exchange-relaxation
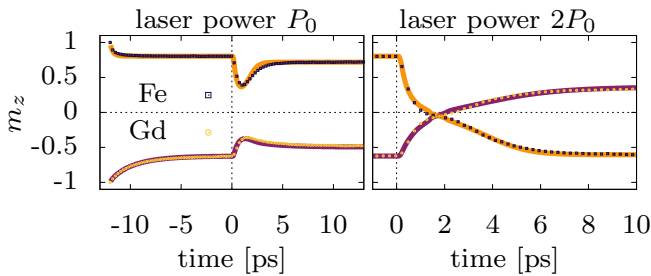
FIG. 6. Element-specific magnetization dynamics of GdFeCo calculated using atomistic spin dynamics (symbols) and the unified phenomenological model derived here, following Eq. (17) (solid lines), for two laser pulse power values (a) P_0 and (b) $2P_0$. Both electron and lattice temperatures are kept constant, $T = 300$ K, for $t < 0$. At $t = 0$, a laser pulse is applied, which is the same as in Fig. 2. GdFeCo alloys with $x_{Gd} = 25\%$ are calculated.

parameter (α_{ex}) as a function of temperature. For the sake of simplicity, the values are those corresponding to the thermal equilibrium. The element-specific relativistic relaxation parameters scale with the value of $\lambda_{a(b)}$ as given in Eq. (15) and depend almost linearly with temperature, with a maximum at the Curie temperature of $2\lambda_{a(b)}/3$. By contrast, the exchange relaxation shows a drastically different behavior. At low temperatures, assuming $\alpha_a = \alpha_b$, one gets $\alpha_{ex} \approx \alpha_a/z$. By contrast, for relatively high temperatures, close to T_c, where $m_{a(b)} \to 0$, α_{ex} scales as $\alpha_{ex} \sim 1/m_a$. Therefore, even at equilibrium, close to the critical temperature, the relaxation dynamics is dominated by exchange-relaxation processes. At nonequilibrium situations, the exchange relaxation can become larger than the relativistic relaxation by driving one of the sublattice magnetization to zero, in principle without the need to approach the critical temperature.

We conduct a direct comparison between the proposed unified and atomistic spin dynamics simulations. The system parameters are exactly the same as those used in the previous sections, when ASD simulations were compared to Baryakhtar and LLB models. The damping parameter is the same for both sublattices, $\lambda_{a(b)} = 0.01$, and we use the same laser powers. We find that the agreement between our unified phenomenological model and ASD simulations is excellent; see Figs. 6(a) and 6(b). Figure 6(a) shows that for $t < 0$, the sublattice magnetization relaxation towards the thermal equilibrium value is described with a high level of accuracy by our model. For $t > 0$ and a relatively low laser power P_0, the agreement is also excellent for the demagnetization and remagnetization dynamics. Figure 6(b) shows the comparison between the unified model and ASD simulations of the switching dynamics. We conclude that Eq. (17) for the sublattice magnetization dynamics, together with Eq. (16) for the effective field and Eqs. (15) and (18) for the relaxation parameters, unify the Baryakhtar and the LLB phenomenological models for single-pulse all-optical switching in ferrimagnets.

Our unified model compares well to ASD simulations for realistic system parameters. For some limiting cases, our model is unable to reproduce ASD simulations. For example, ASD simulations of an isolated ferrimagnet, e.g., no coupling to the heat bath, are impossible to reproduce by our model [14]. This type of sublattice magnetization relaxation has been

named *nondissipative relaxation* since there is no net dissipation into an external bath. All three phenomenological models discussed in this work, i.e., Baryakhtar, LLB, and our unified model, are based on the assumption that the spin system is coupled to a heat bath and they are near thermal equilibrium. Nondissipative relaxation processes could play a role in the exchange relaxation for very low damping values, both nonrealistic and of little interest for ultrafast toggle switching. Nevertheless, we emphasize that the agreement between our model and ASD simulations demonstrates that the potential contribution of internal exchange of angular momentum and energy is minimal for the damping values considered here ($\lambda = 0.01$).

IV. DISCUSSION AND CONCLUSION

The macroscopic model presented in this work solves some open questions in the field of ultrafast magnetization dynamics in ferrimagnets. For example, it answers the question of the range of applicability and the validity of the parameters of the Baryakhtar and LLB phenomenological models. On the one hand, within our model, the relativistic relaxation parameters (α_a) are element specific and strongly depend on both the temperature and the nonequilibrium sublattice magnetization. The temperature and magnetization dependence of the relativistic relaxation parameters are well described by the LLB model. On the other hand, the exchange-relaxation parameter (α_{ex}) is cast in terms of the element-specific relativistic relaxation parameters and sublattice magnetization. We have demonstrated that in order to reproduce the ASD simulations results, the relaxation parameters in the Baryakhtar model have to be both temperature and magnetization dependent. The explicit expression of the exchange-relaxation parameter is the main result of the present work since it allows us to unify the Baryakhtar and LLB models. While for the Baryakhtar model α_e is unconnected to α_a, within our proposed model they are proportional to each other, $\alpha_e \sim \alpha_a/m_a$. This relation is the key to bridge both the ASD simulations and Baryakhtar and LLB models together. Additionally, we have also demonstrated the validity of the nonequilibrium effective fields given in Eq. (16) as derived in the LLB model instead of the Baryakhtar model.

Single-pulse switching in ferrimagnets has been described before by the Baryakhtar model. A necessary condition for switching is that the system transits from the relativistic relaxation regime to the so-called exchange-dominated relaxation regime. Although details of switching in such a regime have already been discussed in detail [5,19], our model resolves the question of how this transition could be described theoretically. When the system is at equilibrium or weakly excited, the exchange-relaxation parameter fulfills $\alpha_e \ll \alpha_a$. For strong excitation, such that the magnetic order of one sublattice reduces significantly close to zero $m_a \to 0$, the exchange relaxation will dominate the dynamics since $\alpha_e \sim \alpha_a/m_a \gg \alpha_a$. From our model, one can derive universal criteria for switching in ferrimagnets, including GdFeCo and Mn_2Ru_xGa [59]. The provided understanding is paramount for further research on material engineering, for example, to find alternative material classes showing all-optical switching. Notably, our model predicts that the exchange-relaxation term is

enhanced as the number of neighbors reduces. This dependence suggests that magnetic systems of lower dimension, e.g., two-dimensional (2D) magnets [60], could show a faster, more efficient switching than bulk materials. Further, the extension of our model to the micromagnetic level will allow one to optimize switching conditions. The use of micromagnetic computational solvers permits a realistic description of ultrafast AOS processes in ferrimagnetic alloys, such as helicity-independent and helicity-dependent AOS, where multidomain states and thermal gradients play an important role in the process [46].

To summarize, in the present work we have presented a unified model for single-pulse all-optical switching in ferrimagnets. Our model merges and improves previous semiphenomenological models, i.e., the Landau-Lifshitz-Bloch model and Baryakhtar-like models. To verify the accuracy of the proposed model, we directly compare the laser-induced magnetization dynamics to atomistic spin dynamics computer simulations. Differently from previous models, our model has the advantage that it can be directly compared to ASD simulations. Further, we have established the connection between ASD and macroscopic equations of motion. Importantly, here we provide a stepping stone for the construction of a micromagnetic model that is valid for ferrimagnets including exchange relaxation between sublattices. This is paramount for a robust construction of a multiscale scheme of the switching process in which not only local magnetization dynamics is described, but also magnetic domain nucleation and motion under strong nonequilibrium. Multiscale-based micromagnetic models will allow for the description of realistic sample sizes and describe recent spintronics phenomena using laser pulses, e.g., magnetic skyrmion creation/deletion with fs laser pulses, or domain-wall motion under dynamics thermal gradients.

[1] C. D. Stanciu, F. Hansteen, A. V. Kimel, A. Kirilyuk, A. Tsukamoto, A. Itoh, and T. Rasing, All-Optical Magnetic Recording with Circularly Polarized Light, Phys. Rev. Lett. **99**, 047601 (2007).

[2] K. Vahaplar, A. M. Kalashnikova, A. V. Kimel, D. Hinzke, U. Nowak, R. Chantrell, A. Tsukamoto, A. Itoh, A. Kirilyuk, and T. Rasing, Ultrafast Path for Optical Magnetization Reversal via a Strongly Nonequilibrium State, Phys. Rev. Lett. **103**, 117201 (2009).

[3] I. Radu, K. Vahaplar, C. Stamm, T. Kachel, N. Pontius, H. A. Dürr, T. A. Ostler, J. Barker, R. F. L. Evans, R. W. Chantrell, A. Tsukamoto, A. Itoh, A. Kirilyuk, T. Rasing, A. V. Kimel, and H. A. Dürr, Transient ferromagnetic-like state mediating ultrafast reversal of antiferromagnetically coupled spins, Nature (London) **472**, 205 (2011).

[4] T. Ostler, J. Barker, R. Evans, R. Chantrell, U. Atxitia, O. Chubykalo-Fesenko, S. El Moussaoui, L. Le Guyader, E. Mengotti, L. Heyderman, F. Nolting, A. Tsukamoto, A. Itoh, D. Afanasiev, B. Ivanov, A. Kalashnikova, K. Vahaplar, J. Mentink, A. Kirilyuk, and T. Rasing, Ultrafast heating as a sufficient stimulus for magnetization reversal in a ferrimagnet, Nat. Commun. **3**, 666 (2012).

[5] J. H. Mentink, J. Hellsvik, D. V. Afanasiev, B. A. Ivanov, A. Kirilyuk, A. V. Kimel, O. Eriksson, M. I. Katsnelson, and T. Rasing, Ultrafast Spin Dynamics in Multisublattice Magnets, Phys. Rev. Lett. **108**, 057202 (2012).

[6] L. Le Guyader, S. El Moussaoui, M. Buzzi, R. V. Chopdekar, L. J. Heyderman, a. Tsukamoto, A. Itoh, A. Kirilyuk, T. Rasing, A. V. Kimel, and F. Nolting, Demonstration of laser induced magnetization reversal in GdFeCo nanostructures, Appl. Phys. Lett. **101**, 022410 (2012).

[7] C. E. Graves, A. H. Reid, T. Wang, B. Wu, S. de Jong, K. Vahaplar, I. Radu, D. P. Bernstein, M. Messerschmidt, L. Müller, R. Coffee, M. Bionta, S. W. Epp, R. Hartmann, N. Kimmel, G. Hauser, A. Hartmann, P. Holl, H. Gorke, J. H. Mentink *et al.*, Nanoscale spin reversal by non-local angular momentum transfer following ultrafast laser excitation in ferrimagnetic GdFeCo., Nat. Mater. **12**, 293 (2013).

[8] J. Barker, U. Atxitia, T. A. Ostler, O. Hovorka, R. W. Chantrell, O. Chubykalo-Fesenko, and R. W. Chantrell, Two-magnon bound state causes ultrafast thermally induced magnetisation switching, Sci. Rep. **3**, 3262 (2013).

[9] V. G. Baryakhtar, V. I. Butrim, and B. A. Ivanov, Exchange relaxation as a mechanism of the ultrafast reorientation of spins in a two-sublattice ferrimagnet, JETP Lett. **98**, 289 (2013).

[10] V. N. Gridnev, Ultrafast heating-induced magnetization switching in ferrimagnets, J. Phys.: Condens. Matter **28**, 476007 (2016).

[11] A. J. Schellekens and B. Koopmans, Microscopic model for ultrafast magnetization dynamics of multisublattice magnets, Phys. Rev. B **87**, 020407(R) (2013).

[12] S. Mangin, M. Gottwald, C.-H. Lambert, D. Steil, V. Uhlíř, L. Pang, M. Hehn, S. Alebrand, M. Cinchetti, G. Malinowski, Y. Fainman, M. Aeschlimann, and E. E. Fullerton, Engineered materials for all-optical helicity-dependent magnetic switching, Nat. Mater. **13**, 286 (2014).

[13] T. A. Ostler, R. F. L. Evans, R. W. Chantrell, U. Atxitia, O. Chubykalo-Fesenko, I. Radu, R. Abrudan, F. Radu, A. Tsukamoto, A. Itoh, A. Kirilyuk, T. Rasing, and A. V. Kimel, Crystallographically amorphous ferrimagnetic alloys: Comparing a localized atomistic spin model with experiments, Phys. Rev. B **84**, 024407 (2011).

[14] S. Wienholdt, D. Hinzke, K. Carva, P. M. Oppeneer, and U. Nowak, Orbital-resolved spin model for thermal magnetization switching in rare-earth-based ferrimagnets, Phys. Rev. B **88**, 020406(R) (2013).

[15] R. Chimata, L. Isaeva, K. Kádas, A. Bergman, B. Sanyal, J. H. Mentink, M. I. Katsnelson, T. Rasing, A. Kirilyuk, A. Kimel,

O. Eriksson, and M. Pereiro, All-thermal switching of amorphous Gd-Fe alloys: Analysis of structural properties and magnetization dynamics, Phys. Rev. B **92**, 094411 (2015).

[16] F. Jakobs, T. A. Ostler, C.-H. Lambert, Y. Yang, S. Salahuddin, R. B. Wilson, J. Gorchon, J. Bokor, and U. Atxitia, Unifying femtosecond and picosecond single-pulse magnetic switching in Gd-Fe-Co, Phys. Rev. B **103**, 104422 (2021).

[17] A. Ceballos, A. Pattabi, A. El-Ghazaly, S. Ruta, C. P. Simon, R. F. L. Evans, T. Ostler, R. W. Chantrell, E. Kennedy, M. Scott, J. Bokor, and F. Hellman, Role of element-specific damping in ultrafast, helicity-independent, all-optical switching dynamics in amorphous (Gd,Tb)Co thin films, Phys. Rev. B **103**, 024438 (2021).

[18] I. Radu, C. Stamm, A. Eschenlohr, F. Radu, R. Abrudan, K. Vahaplar, T. Kachel, N. Pontius, R. Mitzner, K. Holldack, A. Föhlisch, T. A. Ostler, J. H. Mentink, R. F. L. Evans, R. W. Chantrell, A. Tsukamoto, A. Itoh, A. Kirilyuk, A. V. Kimel, and T. Rasing, Ultrafast and Distinct Spin Dynamics in Magnetic Alloys, SPIN **05**, 1550004 (2015).

[19] J. H. Mentink, Manipulating magnetism by ultrafast control of the exchange interaction, J. Phys.: Condens. Matter **29**, 453001 (2017).

[20] U. Atxitia, P. Nieves, and O. Chubykalo-Fesenko, Landau-Lifshitz-Bloch equation for ferrimagnetic materials, Phys. Rev. B **86**, 104414 (2012).

[21] U. Atxitia, T. A. Ostler, J. Barker, R. F. L. Evans, R. W. Chantrell, and O. Chubykalo-Fesenko, Ultrafast dynamical path for the switching of a ferrimagnet after femtosecond heating, Phys. Rev. B **87**, 224417 (2013).

[22] U. Atxitia, J. Barker, R. W. Chantrell, and O. Chubykalo-Fesenko, Controlling the polarity of the transient ferromagnetic-like state in ferrimagnets, Phys. Rev. B **89**, 224421 (2014).

[23] D. Zahn, F. Jakobs, Y. W. Windsor, H. Seiler, T. Vasileiadis, T. A. Butcher, Y. Qi, D. Engel, U. Atxitia, J. Vorberger, and R. Ernstorfer, Lattice dynamics and ultrafast energy flow between electrons, spins, and phonons in a 3d ferromagnet, Phys. Rev. Res. **3**, 023032 (2021).

[24] D. Zahn, F. Jakobs, H. Seiler, T. A. Butcher, D. Engel, J. Vorberger, U. Atxitia, Y. W. Windsor, and R. Ernstorfer, Intrinsic energy flow in laser-excited 3d ferromagnets, Phys. Rev. Res. **4**, 013104 (2022).

[25] B. Frietsch, J. Bowlan, R. Carley, M. Teichmann, S. Wienholdt, D. Hinzke, U. Nowak, K. Carva, P. M. Oppeneer, and M. Weinelt, Disparate ultrafast dynamics of itinerant and localized magnetic moments in gadolinium metal, Nat. Commun. **6**, 8262 (2015).

[26] B. Frietsch, A. Donges, R. Carley, M. Teichmann, J. Bowlan, K. Döbrich, K. Carva, D. Legut, P. M. Oppeneer, U. Nowak, and M. Weinelt, The role of ultrafast magnon generation in the magnetization dynamics of rare-earth metals, Sci. Adv. **6**, eabb1601 (2020).

[27] E. Iacocca, T.-M. M. Liu, A. H. Reid, Z. Fu, S. Ruta, P. W. Granitzka, E. Jal, S. Bonetti, A. X. Gray, C. E. Graves, R. Kukreja, Z. Chen, D. J. Higley, T. Chase, L. Le Guyader, K. Hirsch, H. Ohldag, W. F. Schlotter, G. L. Dakovski, G. Coslovich *et al.*, Spin-current-mediated rapid magnon localisation and coalescence after ultrafast optical pumping of ferrimagnetic alloys, Nat. Commun. **10**, 1756 (2019).

[28] U. Atxitia, T. A. Ostler, R. W. Chantrell, and O. Chubykalo-Fesenko, Optimal electron, phonon, and magnetic characteristics for low energy thermally induced magnetization switching, Appl. Phys. Lett. **107**, 192402 (2015).

[29] U. Atxitia and T. A. Ostler, Ultrafast double magnetization switching in GdFeCo with two picosecond-delayed femtosecond pump pulses, Appl. Phys. Lett. **113**, 062402 (2018).

[30] C. Xu, T. A. Ostler, and R. W. Chantrell, Thermally induced magnetization switching in Gd/Fe multilayers, Phys. Rev. B **93**, 054302 (2016).

[31] S. Gerlach, L. Oroszlany, D. Hinzke, S. Sievering, S. Wienholdt, L. Szunyogh, and U. Nowak, Modeling ultrafast all-optical switching in synthetic ferrimagnets, Phys. Rev. B **95**, 224435 (2017).

[32] C. Banerjee, N. Teichert, K. E. Siewierska, Z. Gercsi, G. Y. P. Atcheson, P. Stamenov, K. Rode, J. M. D. Coey, and J. Besbas, Single pulse all-optical toggle switching of magnetization without gadolinium in the ferrimagnet Mn_2Ru_xGa, Nat. Commun. **11**, 4444 (2020).

[33] C. Banerjee, K. Rode, G. Atcheson, S. Lenne, P. Stamenov, J. M. D. Coey, and J. Besbas, Ultrafast Double Pulse All-Optical Reswitching of a Ferrimagnet, Phys. Rev. Lett. **126**, 177202 (2021).

[34] F. Jakobs and U. Atxitia, Atomistic spin model of single pulse toggle switching in Mn_2Ru_xGa Heusler alloys, Appl. Phys. Lett. **120**, 172401 (2022).

[35] V. G. Baryakhtar and A. G. Danilevich, The phenomenological theory of magnetization relaxation (Review article), Low Temp. Phys. **39**, 993 (2013).

[36] E. Lifshits and L. Landau, On the theory of dispersion of magnetic permeability in ferromagnetic bodies, Phys. Zeitsch. der Sow. **8**, 153 (1935).

[37] A. Kamra, R. E. Troncoso, W. Belzig, and A. Brataas, Gilbert damping phenomenology for two-sublattice magnets, Phys. Rev. B **98**, 184402 (2018).

[38] C. S. Davies, T. Janssen, J. H. Mentink, A. Tsukamoto, A. V. Kimel, A. F. G. van der Meer, A. Stupakiewicz, and A. Kirilyuk, Pathways for Single-Shot All-Optical Switching of Magnetization in Ferrimagnets, Phys. Rev. Appl. **13**, 024064 (2020).

[39] C. S. Davies, G. Bonfiglio, K. Rode, J. Besbas, C. Banerjee, P. Stamenov, J. M. D. Coey, A. V. Kimel, and A. Kirilyuk, Exchange-driven all-optical magnetic switching in compensated 3d ferrimagnets, Phys. Rev. Res. **2**, 032044(R) (2020).

[40] D. A. Garanin, Fokker-Planck and Landau-Lifshitz-Bloch equations for classical ferromagnets, Phys. Rev. B **55**, 3050 (1997).

[41] O. Chubykalo-Fesenko, U. Nowak, R. W. Chantrell, and D. Garanin, Dynamic approach for micromagnetics close to the Curie temperature, Phys. Rev. B **74**, 094436 (2006).

[42] P. Nieves, D. Serantes, U. Atxitia, and O. Chubykalo-Fesenko, Quantum Landau-Lifshitz-Bloch equation and its comparison with the classical case, Phys. Rev. B **90**, 104428 (2014).

[43] U. Atxitia, D. Hinzke, and U. Nowak, Fundamentals and applications of the Landau-Lifshitz-Bloch equation, J. Phys. D **50**, 033003 (2017).

[44] M. Hennecke, I. Radu, R. Abrudan, T. Kachel, K. Holldack, R. Mitzner, A. Tsukamoto, and S. Eisebitt, Angular Momentum Flow During Ultrafast Demagnetization of a Ferrimagnet, Phys. Rev. Lett. **122**, 157202 (2019).

[45] C. Vogler, C. Abert, F. Bruckner, and D. Suess, Stochastic ferrimagnetic Landau-Lifshitz-Bloch equation for finite magnetic structures, Phys. Rev. B **100**, 054401 (2019).

[46] V. Raposo, F. García-Sánchez, U. Atxitia, and E. Martínez, Realistic micromagnetic description of all-optical ultrafast switching processes in ferrimagnetic alloys, Phys. Rev. B **105**, 104432 (2022).

[47] F. Schlickeiser, U. Ritzmann, D. Hinzke, and U. Nowak, Role of Entropy in Domain Wall Motion in Thermal Gradients, Phys. Rev. Lett. **113**, 097201 (2014).

[48] S. Moretti, V. Raposo, E. Martinez, and L. Lopez-Diaz, Domain wall motion by localized temperature gradients, Phys. Rev. B **95**, 064419 (2017).

[49] S. Lepadatu, Emergence of transient domain wall skyrmions after ultrafast demagnetization, Phys. Rev. B **102**, 094402 (2020).

[50] J. Barker and U. Atxitia, A Review of Modelling in Ferrimagnetic Spintronics, J. Phys. Soc. Jpn. **90**, 081001 (2021).

[51] R. Chimata, A. Bergman, L. Bergqvist, B. Sanyal, and O. Eriksson, Microscopic Model for Ultrafast Remagnetization Dynamics, Phys. Rev. Lett. **109**, 157201 (2012).

[52] U. Nowak, Classical spin models in *Handbook of Magnetism and Advanced Magnetic Materials*, edited by H. Kronmller, S. Parkin, J. E. Miltat, and M. R. Scheinfein (Wiley, New York, 2007).

[53] U. Atxitia, O. Chubykalo-Fesenko, R. W. Chantrell, U. Nowak, and A. Rebei, Ultrafast Spin Dynamics: The Effect of Colored Noise, Phys. Rev. Lett. **102**, 057203 (2009).

[54] D. Hinzke, U. Atxitia, K. Carva, P. Nieves, O. Chubykalo-Fesenko, P. M. Oppeneer, and U. Nowak, Multiscale modeling of ultrafast element-specific magnetization dynamics of ferromagnetic alloys, Phys. Rev. B **92**, 054412 (2015).

[55] Y. Yang, R. B. Wilson, J. Gorchon, C.-H. Lambert, S. Salahuddin, and J. Bokor, Ultrafast magnetization reversal by picosecond electrical pulses, Sci. Adv. **3**, e1603117 (2017).

[56] M. I. Kaganov, I. M. Lifshitz, and L. V. Tanatarov, Relaxation between electrons and crystalline lattices, Sov. Phys. JETP **4**, 173 (1957).

[57] J. Chen, D. Tzou, and J. Beraun, A semiclassical two-temperature model for ultrafast laser heating, Intl. J. Heat Mass Transf. **49**, 307 (2006).

[58] U. Atxitia, O. Chubykalo-Fesenko, J. Walowski, A. Mann, and M. Münzenberg, Evidence for thermal mechanisms in laser-induced femtosecond spin dynamics, Phys. Rev. B **81**, 174401 (2010).

[59] F. Jakobs and U. Atxitia, Universal Criteria for Single Femtosecond Pulse Ultrafast Magnetization Switching in Ferrimagnets, Phys. Rev. Lett. **129**, 037203 (2022).

[60] Q. H. Wang, A. Bedoya-Pinto, M. Blei, A. H. Dismukes, A. Hamo, S. Jenkins, M. Koperski, Y. Liu, Q.-C. Sun, E. J. Telford, H. H. Kim, M. Augustin, U. Vool, J.-X. Yin, L. H. Li, A. Falin, C. R. Dean, F. Casanova, R. F. L. Evans, M. Chshiev *et al.*, The magnetic genome of two-dimensional van der Waals materials, ACS Nano **16**, 6960 (2022).